

Remote Control of Time-Regulated Stretching of Ligand-Presenting Nanocoils In Situ Regulates the Cyclic Adhesion and Differentiation of Stem Cells

Sunhong Min, Min Jun Ko, Hee Joon Jung, Wonsik Kim, Seong-Beom Han, Yuri Kim, Gunhyu Bae, Sungkyu Lee, Ramar Thangam, Hyojun Choi, Na Li, Jeong Eun Shin, Yoo Sang Jeon, Hyeon Su Park, Yu Jin Kim, Uday Kumar Sukumar, Jae-Jun Song, Seung-Keun Park, Seung-Ho Yu, Yun Chan Kang, Ki-Bum Lee, Qiang Wei, Dong-Hwee Kim, Seung Min Han, Ramasamy Paulmurugan, Young Keun Kim,* and Heemin Kang*

Native extracellular matrix (ECM) can exhibit cyclic nanoscale stretching and shrinking of ligands to regulate complex cell–material interactions. Designing materials that allow cyclic control of changes in intrinsic ligand-presenting nanostructures in situ can emulate ECM dynamicity to regulate cellular adhesion. Unprecedented remote control of rapid, cyclic, and mechanical stretching (“ON”) and shrinking (“OFF”) of cell-adhesive RGD ligand-presenting magnetic nanocoils on a material surface in five repeated cycles are reported, thereby independently increasing and decreasing ligand pitch in nanocoils, respectively, without modulating ligand-presenting surface area per nanocoil. It is demonstrated that cyclic switching “ON” (ligand nanostretching) facilitates time-regulated integrin ligation, focal adhesion, spreading, YAP/TAZ mechanosensing, and differentiation of viable stem cells, both in vitro and in vivo. Fluorescence resonance energy transfer (FRET) imaging reveals magnetic switching “ON” (stretching) and “OFF” (shrinking) of the nanocoils inside animals. Versatile tuning of physical dimensions and elements of nanocoils by regulating electrodeposition conditions is also demonstrated. The study sheds novel insight into designing materials with connected ligand nanostructures that exhibit nanocoil-specific nano-spaced declustering, which is ineffective in nanowires, to facilitate cell adhesion. This unprecedented, independent, remote, and cytocompatible control of ligand nanopitch is promising for regulating the mechanosensing-mediated differentiation of stem cells in vivo.

1. Introduction

Native extracellular matrix (ECM) can regulate the interactions between cells and ligands by exerting nanoscale and cyclic stretching and shrinking of ligands, such as Arg–Gly–Asp (RGD) ligand, in various tissues and organs (including bone,^[1] muscle,^[2] and heart^[3]) in vivo. Cyclic stretching of cell-adhesive ECM proteins, such as collagen, can mediate the spreading and mechanotransduction of adherent cells by facilitating dynamic binding of integrin receptor to RGD ligand to stimulate the organization of cytoskeletal actin and focal adhesion complexes. Furthermore, it has been reported that cyclic mechanical loading to native bone tissue significantly enhanced bone formation rate.^[1] Designing novel materials that allow remote, in situ, and cyclic control of nanoscale stretching and shrinking of ligand presentation can emulate native bone ECM microenvironment^[4] to help unravel dynamic and nanoscale cell–ligand interactions in vivo and effectively regulate dynamic cellular adhesion, mechanotransduction, and differentiation.^[5]

S. Min, M. J. Ko, Y. Kim, G. Bae, S. Lee, Dr. R. Thangam, H. Choi, Dr. J. E. Shin, Dr. Y. S. Jeon, H. S. Park, Dr. Y. J. Kim, Prof. Y. C. Kang, Prof. Y. K. Kim, Prof. H. Kang
Department of Materials Science and Engineering
Korea University
Seoul 02841, Republic of Korea
E-mail: ykim97@korea.ac.kr; heeminkang@korea.ac.kr

Dr. H. J. Jung
Department of Materials Science and Engineering
Northwestern University
Evanston, IL 60208, USA

Dr. H. J. Jung
International Institute for Nanotechnology
Evanston, IL, USA

Dr. H. J. Jung
NUANCE Center
Northwestern University
Evanston, IL, USA

 The ORCID identification number(s) for the author(s) of this article can be found under <https://doi.org/10.1002/adma.202008353>.

DOI: 10.1002/adma.202008353

Remote and active control of ECM-mimicking ligand-nano-engineered materials^[6] using various stimuli^[7] can regulate and elucidate dynamic interactions between cells and nanoscale ligands at the molecular level, thereby benefiting the advancement of safe patient-tailorable therapies.^[8,9] A recent study showed that the application of negative and positive electric potentials to materials suppressed and facilitated cell adhesion, respectively, by controlling RGD accessibility.^[10] Light illumination^[11,12] has been utilized to activate light-responsive materials to temporally modulate cell adhesion and differentiation^[13] through ligand photocleavage,^[13–15] photoisomerization,^[16,17] or photothermal effect.^[18] It has been recently that NIR light irradiation in different intensities can modulate photoisomerization^[16] to regulate cell adhesion or photocleavage to regulate stem cell differentiation into adipocytes or osteoblasts.^[15] High-strength tissue-penetrating magnetic fields^[19] (7 T) have been safely used on patients.^[20] In our other studies, we utilized magnetic nanoparticles to magnetically control their alignment,^[21]

sliding,^[22] macroscale movement,^[23] or ligand uncaging,^[24] to dynamically regulate cellular adhesion.^[25] However, none of the previous studies have demonstrated the remote, in situ, and cyclic control of structural changes in nanomaterial themselves coated with ligand to reversibly regulate cellular adhesion both in vitro and in vivo.

In this present study, we report for the first time that magnetic control of cyclic and nanoscale stretching (“ON”) and shrinking (“OFF”) of RGD ligand-presenting nanocoils on material surface in situ regulates stem cell adhesion both in vitro and in vivo (**Scheme 1**). Electrodeposition condition-regulated development of such uniquely shaped^[26,27] ligand CoFe nanocoils enabled the magnetic and independent manipulation of intrinsic changes in their nanodimensions (i.e., ligand pitch in the nanocoils). We confirmed that the wire diameter and outer nanocoil diameter of the ligand-bearing nanocoils remained constant in the presence and absence of magnetic field, thereby suggesting constant ligand-presenting surface area per nanocoil and thus constant macroscale ligand density irrespective of magnetic field application. Our present study utilizing remote control of intrinsic changes in magnetic ligand nanodimensions is in contrast with prior studies, in which the movement of spherical nanoparticles^[22,24,28,29] was exploited without their nanostructural changes. Our present study utilizes structural changes of magnetic ligand-presenting nanocoils and is thus different from previous studies demonstrating the modulation of spacing^[30] with dynamic changes,^[29,31] cluster size and density,^[32] ordering,^[33] and local versus global density^[34] of ligand-bearing spherical nanomaterials^[35,36] or micropatterns^[37] that do not change their intrinsic structures.

We demonstrate the magnetic switching “ON” (i.e., stretching of ligand-presenting nanocoils) that independently increases intra-nanocoil ligand pitch (without modulating ligand-presenting nanocoil surface area), which facilitated viable stem cell adhesion and mechanosensing in repeated cycles and consequential stem cell differentiation both in vitro and in vivo (**Scheme 1**). Thus, it is beneficial to design materials with connected ligand nanostructures that are slightly nano-spaced (i.e., declustered) to promote cell adhesion. The surfaces of nanocoils are not completely flat and thus partially anchored to material surfaces, which enabled cyclic stretching and shrinking of non-material-anchored surfaces of nanocoils. This unprecedented, independent, and remote control of ligand nanopitch can be a breakthrough in designing novel materials to regulate stem cell adhesion and subsequent differentiation in vivo for enabling regenerative therapies.

2. Results and Discussion

To remotely control the changes in the intrinsic ligand nanostructures without modulating ligand-presenting surface area per nanostructure, we developed magnetic CoFe nanocoils via tuning of nanoporous template-assisted electrodeposition conditions by including vanadium oxide ions and ascorbic acid in single mixed metal precursor solution (**Figure S1**, Supporting Information). We present versatile tuning of physical dimensions (length and diameter) of CoFe nanocoils and elements of Co nanocoils by regulating electrodeposition conditions,

W. Kim, Prof. S. M. Han

Department of Materials Science and Engineering
Korea Advanced Institute of Science and Technology
Daejeon 34141, Republic of Korea

N. Li, Prof. J.-J. Song

Department of Otorhinolaryngology-Head and Neck Surgery
Korea University College of Medicine
Seoul 08308, Republic of Korea

Dr. U. K. Sukumar, Prof. R. Paulmurugan

Department of Radiology
Molecular Imaging Program at Stanford
Stanford University School of Medicine
Stanford University
Palo Alto, CA 94304, USA

Prof. S.-K. Park

Department of Chemical Engineering
Kongju National University
Cheonan 31080, Republic of Korea

Prof. S.-H. Yu

Department of Chemical and Biological Engineering
Korea University
Seoul 02841, Republic of Korea

Prof. K.-B. Lee

Department of Chemistry and Chemical Biology
Rutgers University
Piscataway, NJ 08854, USA

Prof. Q. Wei

College of Polymer Science and Engineering
State Key Laboratory of Polymer Materials and Engineering
Sichuan University
Chengdu 610065, China

Prof. D.-H. Kim, S.-B. Han

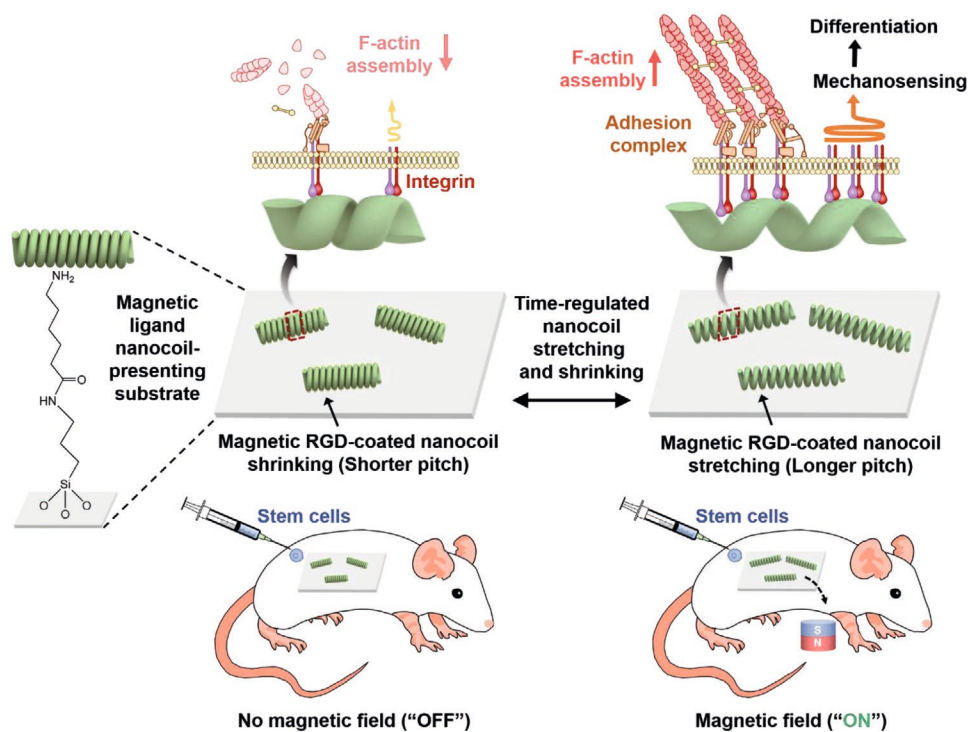
KU-KIST Graduate School of Converging Science and Technology
Korea University
Seoul 02841, Republic of Korea

Prof. R. Paulmurugan

Department of Radiology
Canary Center at Stanford for Cancer Early Detection
Stanford University School of Medicine
Stanford University
Palo Alto, CA 94304, USA

Prof. Y. K. Kim, Prof. H. Kang

Department of Biomicrosystem Technology
Korea University
Seoul 02841, Republic of Korea



Scheme 1. Schematic illustration of the methodology in this study. Magnetic control of time-regulated stretching (“ON”) and shrinking (“OFF”) of ligand-presenting nanocoils in situ on material surfaces while maintaining a similar ligand surface area per nanocoil and thus constant macroscale ligand density. Magnetic switching “ON” (i.e., stretching of ligand-presenting nanocoils) facilitated cyclic adhesion and mechanosensing of stem cells, both in vitro and in vivo, and their consequential differentiation.

such as deposition time, template pore size, and single cobalt-containing precursor solution, respectively. High-angle annular dark-field scanning transmission electron microscopy (HAADF-STEM) with energy-dispersive spectra and mapping as well as electron energy loss spectra and mapping collectively confirmed helical shape of nanocoils with homogeneous distribution of Co and Fe elements with an average composition of $\text{Co}_{50}\text{Fe}_{50}$ at.% (Figures 1a and Figures S2 and S3, Supporting Information). High-resolution STEM (HR-STEM) at atomic resolution, HR-TEM, and X-ray diffraction (XRD) spectra collectively confirmed periodic lattice fringes with average lattice spacing of 2.02 ± 0.02 Å, corresponding to (110) plane in body-centered cubic crystal structure of CoFe phase in nanocoils (Figures S4, S5, and S6, Supporting Information). Vibrating sample magnetometry (VSM) confirmed reversible magnetic properties of CoFe nanocoils, thereby enabling reversible magnetic switching of “ON” (stretching) and “OFF” (shrinking) (Figure 1b). We demonstrate for the first time in situ tensile loading measurements of the “nanocoils” using Push-to-Pull device with SEM-FIB dual beam system.^[38] We showed that the nanocoil is elastically elongated without fracture up to 1.57 ± 0.21 GPa at strain of 0.024 ± 0.001 (Figure 1c and Figure S10a,b).

Next, to enable in situ time-regulated stretching and shrinking of ligand-bearing nanocoils on material surface, we functionalized and chemically coupled the magnetic nanocoils to material surfaces. Fourier transform infrared spectra revealed successful coupling of aminocaproic acid and PEGylated RGD peptides to the nanocoils via the carboxylate group and amide

bond, respectively (Figure S7, Supporting Information). The carboxylate group on nanocoils was grafted to aminated material surfaces. Thiolated RGD peptide ligand was subsequently coupled to the nanocoil surfaces via poly(ethylene glycol) (PEG) linker (Figure S8, Supporting Information). To minimize non-ligand-specific cell adhesion, non-nanocoil-covered areas were PEGylated. Scanning electron microscopy (SEM) images in low and high magnifications confirmed homogeneously distributed material-coupled ligand-bearing nanocoils at a density of approximately 59955 ± 5984 nanocoils per mm^2 (Figures 1d and Figure S9, Supporting Information). Compared to relevant references utilizing ligand-presenting gold nanoparticles (approximately 8–10 nm) that promoted cell adhesion in the ligand spacing below 70 nm,^[29,33,34,39] we used the substrate with relatively higher ligand spacing between the bigger ligand-presenting nanocoils since it allowed clear elucidation of the effect of magnetic switching of ligand nanostretching and nanoshrinking on effectively regulating time-regulated mechanosensing-dependent differentiation of stem cells.

We next characterized reversible magnetic switching “ON” (stretching) and “OFF” (shrinking) of ligand-presenting nanocoils without modulating ligand-presenting surface area per nanocoil via in situ magnetic atomic force microscopy (AFM) imaging. Serial AFM imaging of scanning identical areas clearly revealed that placing a permanent magnet near the edge of materials promoted stretching of the ligand-presenting nanocoils in situ toward the edge of the materials (“ON”) and removing the magnet induced their reversible shrinking to the original nanostructures (“OFF”) (Figure 1e,f). Linear

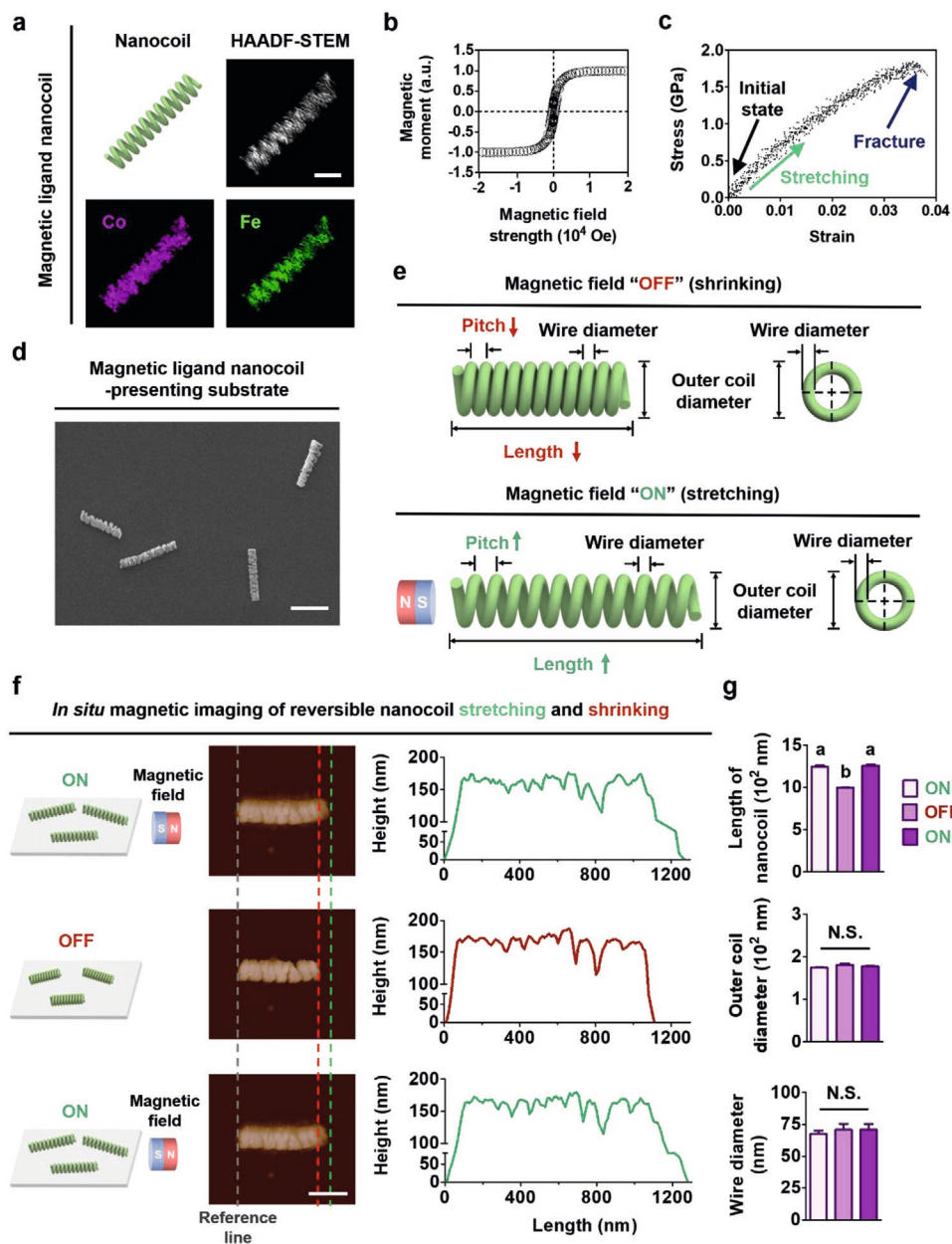


Figure 1. Remote control of reversible stretching (“ON”) and shrinking (“OFF”) of ligand-bearing nanocoils without modulating the ligand surface area per nanocoil. a) HAADF-STEM, elemental mapping, b) VSM hysteresis, and c) stress–strain curve (under *in situ* tensile loading) of CoFe nanocoils. The magnetic moment is normalized to the maximum value of the magnetic moment as a function of magnetic field strength. d) SCM-SCM of material-coupled ligand-bearing nanocoils. e) Schematic illustration and f) *in situ* magnetic AFM of ligand-bearing nanocoils partially covalently anchored to material surfaces under reversible magnetic switching “ON” and “OFF” with linear height profiles and g) quantification of the length, outer diameter, and wire diameter of ligand-bearing nanocoils. Scale bars: 250 nm (HAADF-STEM and elemental mapping), 1 μ m (SEM), and 500 nm (AFM).

height profiles along the axis of nanocoils were used to quantify nanoscale dimensions under cyclic magnetic switching (“ON”, “OFF”, and “ON”) (Figure 1g). The outer nanocoil diameter remained nearly constant (from 174 to 180 nm with no significant differences) during cyclic switching. The wire diameter also remained constant (from 66 to 71 nm with no significant differences). These suggest that ligand-presenting surface areas of each nanocoil and thus macroscale ligand density remain constant during cyclic switching. We designed their dimensions to be similar to the size of integrin receptors

(\approx 10 nm) to allow each ligand-presenting coil-specific isotropic integrin recruitment.^[40] In stark contrast, the nanocoil length exhibited significantly different changes from 1241 ± 28 nm (“ON”) to 995 ± 4 nm (“OFF”) to 1255 ± 18 nm (“ON”), which accordingly enable an increase (“ON”) and decrease (“OFF”) in the pitch of ligand-presenting nanocoil. The magnetically controlled cyclic stretching and shrinking of the ligand-presenting nanocoils were visualized and quantified in “two repeated cycles” (“OFF–ON–OFF–ON–OFF”), which accordingly enabled consistent increase (“ON”) and decrease (“OFF”) in the pitch

of ligand-presenting nanocoil (Figure S11a,b, Supporting Information). As control experiments, static serial AFM imaging of identical areas without the magnet exhibited negligible structural changes in nanocoil (Figure S12, Supporting Information).

We conducted in situ magnetic confocal microscopy imaging for “real-time” monitoring of magnetically controlled motion of the nanocoils for the first time. We showed that the ligand-presenting nanocoils exhibit rapid cyclic stretching (expansion, magnet “ON”) within 30 s and shrinking (magnet “OFF”) within 30 s for “5 repeated cycles”, which were intact (Movie S1, Supporting Information). The faint black (defocused) color in the shrinking (“OFF”) condition emerged at the majority part of the nanocoil (that appears to be bent out of the plane) and the clear black (focused) color in the stretching (“ON”) condition emerged across the whole nanocoil (that appears to be straightened). These findings may suggest that the nanocoil is partially and covalently coupled to material surface to enable cyclic stretching and shrinking of non-coupled surfaces of nanocoils on material surface. Furthermore, we simultaneously imaged the ligand-presenting nanocoils and adherent stem cells for 6 h, which revealed that the ligand-presenting nanocoils were intact (not internalized by the cells) (Movie S2, Supporting Information).

Next, we examined whether remote control of time-regulated switching “ON” (stretching) and “OFF” (shrinking) of ligand-bearing nanocoils can regulate cyclic adhesion of human mesenchymal stem cells (hMSCs).^[41,42] Immunofluorescence revealed that magnetic switching “ON” facilitated significantly higher adherent cell density and focal adhesion over a wider area and vinculin clustering in focal adhesion complexes than magnetic switching “OFF” (Figure S13a,b, Supporting Information). Cyclic switching “ON” (stretching) and “OFF” (shrinking) of ligand-bearing nanocoils promoted and inhibited time-regulated integrin $\beta 1$ expression and focal adhesion of stem cells, respectively, in repeated cycles (Figures 2a and Figure S14, Supporting Information). We believe the magnetic switching “ON” facilitates integrin $\beta 1$ ligation to the RGD ligand-presenting stretched nanocoils that mediates focal adhesion (vinculin clusters) assembly, thereby facilitating F-actin assembly of stem cells. As control experiments, we prepared two different CoFe nanocoils and two different CoFe (non-coiled) nanowires in 1.0 and 1.3 μm lengths and coupled them to the substrate (Figures S15a,b and S16a,b). We found that 1.0 μm -long ligand-presenting nanocoils in the magnetic “ON” condition (that are stretched to 1.3 μm in length) exhibited similar levels of cell adhesion compared to 1.3 μm -long ligand-presenting nanocoils in the “OFF” condition and higher levels of cell adhesion compared to 1.0 μm -long ligand-presenting nanocoils in the “OFF” conditions (Figures S17 and S18). In stark contrast, we found that 1.3 μm -long (non-coiled) nanowires did not significantly promote cell adhesion compared with 1.0 μm -long nanowires, suggesting that the cell adhesion promoted by the magnetically controlled increase in the length in the nanocoil in the “ON” condition was nanocoil shape-specific regulation. We found that magnetic switching “ON” (stretching) and “OFF” (shrinking) of CoFe nanocoils were not cytotoxic to adherent stem cells with nearly all cells alive after 48 h, which proves their cytocompatibility (Figure S19a,b, Supporting Information). As control experiments, minimal cell adhesion occurred

with no significant differences under magnetic switching “ON” and “OFF” in the absence of RGD ligand or nanocoils, proving the necessity of both RGD ligand and nanocoils to support and remotely regulate stem cell adhesion (Figure S20a,b, Supporting Information).

Interestingly, these findings suggest that slightly nano-spaced declustering (according to increasing ligand nanopitch) of the connected ligand nanostructures (e.g., ligand-presenting nanocoils) under magnetic switching “ON” (nanostretching) without modulating ligand-presenting surface area activates cell adhesion, which sheds an insight into novel design of materials. We are currently investigating the effect of modulation of nanocoil pitch and wire diameter by modulating the amount of metal precursor and current density on magnetic switching-regulated cell adhesion. Furthermore, we used a magnet with higher magnetic strength (approximately 2 T) than 270 mT used in this study and found no significant increase in ligand nanopitch (data not shown). This suggests that our magnetic control of nanostretching will be consistent in tesla-scale magnetic applications currently used in clinical setting.

The integrin ligation-mediated focal adhesion and spreading of stem cells activate mechanotransduction signaling that can mediate stem cell differentiation.^[43–45] It has been reported that cyclic mechanical loading to native bone markedly elevated bone formation rate.^[1] Therefore, we investigated whether such natural effect is consistently applicable to the effect of our remote and time-regulated switching “ON” (nanostretching) and “OFF” (nanoshrinking) on osteogenic differentiation of stem cells. We found that time-regulated magnetic switching “ON” (nanostretching) stimulates significantly higher nuclear translocation of YAP mechanotransducers^[46] of stem cells (including “OFF–ON–OFF” and “ON–OFF–ON” groups) in a reversible manner (Figure 2b and Figure S21, Supporting Information). We also found that temporal magnetic switching “ON” (nanostretching) reversibly facilitates higher nuclear TAZ translocation and pronounced expression of early markers (significantly higher alkaline phosphatase-positive cells, RUNX2/ALP gene expression, nuclear translocation in RUNX2, and late marker (pronounced osteocalcin expression) for osteogenic differentiation in stem cells (Figures 2c and Figures S22a,b, S23, S24 and S25a,b, Supporting Information). We next found that magnetic switching “ON”-induced mechanosensing of stem cells involves signaling molecules, such as myosin II, rho-associated protein kinase (ROCK), and actin polymerization, which positively regulate pronounced nuclear localization of YAP/TAZ mechanotransducers (Figures S26a,b and S27a,b). Taken together, magnetic switching “ON” mediates stem cell differentiation through YAP/TAZ mechanotransduction.

We next investigated whether our proven remote and time-regulated switching “ON” (nanostretching)-facilitated mechanosensing-mediated differentiation of stem cells remains effective in vivo with host cells. We implanted materials presenting ligand-bearing nanocoils into subcutaneous pockets of nude mice and then injected hMSCs onto the materials (Figure 3a). We placed the magnet near the edge of the materials (on the abdomen side) (“ON”) or removed (“OFF”) it to establish time-regulated switching. We performed in vivo fluorescence resonance energy transfer (FRET) imaging to verify reversible stretching of the nanocoils under magnetic control for the first

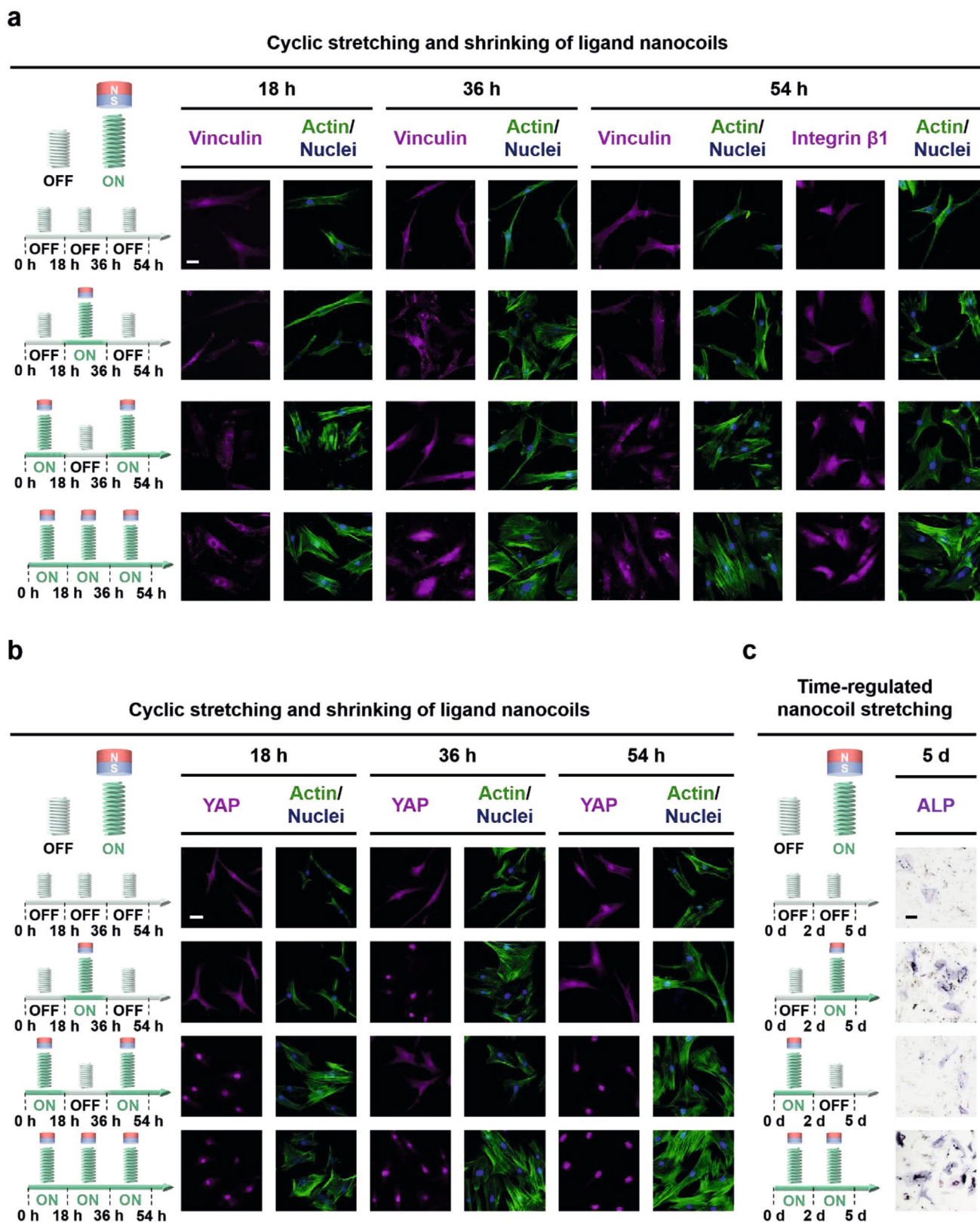


Figure 2. Cyclic magnetic switching “ON” for ligand nanostretching in situ promotes time-regulated adhesion, mechanosensing, and differentiation of stem cells. a–c) Immunofluorescence for F-actin and nuclei with vinculin (a), YAP (b), and ALP (c) staining of adherent stem cells under cyclic switching “ON” and “OFF”. Scale bars: 50 μm .

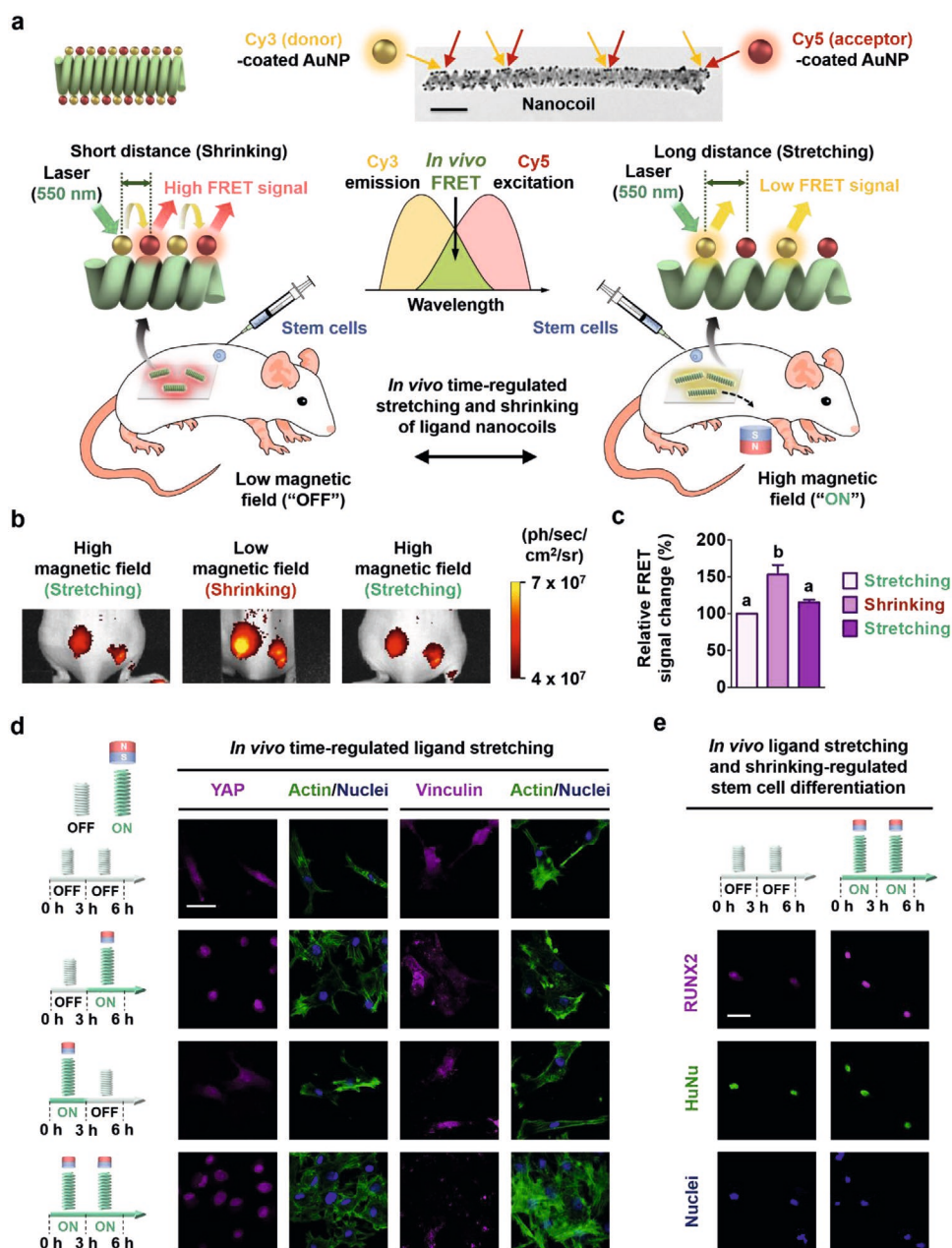


Figure 3. In vivo time-regulated “ON” to induce ligand nanostretching facilitates mechanosensing-mediated differentiation of stem cells. a) Schematic representation of subcutaneous implantation and injection of stem cells under magnetic field. b,c) Transmission electron microscopy of the Au(Cy3 donor)–Au(Cy5 acceptor)–nanocoils used for in vivo FRET imaging (b) and signal quantification (c). Scale bar: 500 nm. d) Immunofluorescence for YAP and vinculin with actin and nuclei and e) RUNX2 with human-specific HuNu and nuclei in stem cells injected onto subcutaneously implanted materials under time-regulated magnetic switching “ON” and “OFF”. Scale bars: 50 μ m.

time. We coupled the first set of Au nanoparticles (AuNPs) to the nanocoils and coated the first set of AuNPs with amino-Cy3 fluorescent dye (donor). We then coupled the second set of AuNPs to the nanocoils and then coated the second set of AuNPs with amino-Cy5 fluorescent dye (acceptor) to prepare Au(Cy3)–Au(Cy5)–nanocoils. We confirmed size uniformity of the AuNPs used for nanocoil coupling via TEM imaging and DLS analysis (Figure S28a,c, Supporting Information). We imaged significantly lower FRET signals under high magnetic field inducing the stretching of the implanted the

Au(Cy3)–Au(Cy5)–nanocoils compared to low magnetic field inducing their shrinking (Figure 3a–c).

By immunofluorescent staining, we also confirmed the injected hMSCs that had adhered to the materials by detecting co-localization of human-specific nuclear antigen (HuNu) and DAPI-positive nuclei in all groups (Figure S29, Supporting Information). Immunofluorescence confirmed that in vivo time-regulated switching “ON” (“OFF–ON” and “ON–ON” groups) stimulates significantly higher adherent density and focal adhesion of stem cells over a wider area and vinculin clustering, and

YAP mechanotransduction (Figure 3d and Figure S30, Supporting Information). We also found that in vivo switching “ON” facilitates significantly higher nuclear translocation of RUNX2 co-localized with HuNu, thereby stimulating osteogenic differentiation (i.e., normal physiological function) of stem cells in vivo, coexistent with adhered host immune cells (NIMP-R14-positive neutrophils) (Figure 3e and Figures S31 and S32a,b, Supporting Information). Co and Fe elements naturally exist as ions in the body. A recent study has demonstrated that CoFe-based nanomaterials exhibit no systemic toxicity to various organs, such as brain, kidney, lung, liver, and spleen and their functionality in vivo.^[47] SEM imaging of the nanocoil-coated substrate after implantation into mice (under magnetic switching “ON” and “OFF”) revealed that the nanocoils were intact inside the animals (Figure S33, Supporting Information). Therefore, our time-regulated stretching of ligand-presenting CoFe nanocoils in situ offers unprecedented opportunities in safe, remote, and effective control of mechanosensing-dependent stem cell differentiation over prolonged time for potential regenerative therapies.

3. Conclusion

In summary, we tune electrodeposition conditions to develop CoFe nanocoils and chemically couple them to material surfaces to allow unprecedented, remote, and in situ control of cyclic nanoscale stretching (“ON”) and shrinking (“OFF”) of ligand-presenting magnetic nanocoils, which independently increases and decreases ligand pitch in nanocoils, respectively. This magnetic switching “ON” and “OFF” maintains both outer nanocoil diameter and wire diameter constant, thereby keeping both ligand-presenting surface area per nanocoil and macroscale ligand density invariant. We demonstrate that magnetic switching “ON” (ligand nostretching) promotes cytocompatible focal adhesion, spreading, and mechanotransduction of stem cells in repeated cycles that facilitate their consequential differentiation both in vitro and in vivo. Magnetic switching “ON”-mediated YAP/TAZ mechanosensing of stem cells involves signaling molecules, such as myosin II, ROCK, and actin polymerization. These findings can be applied to design novel materials presenting slightly nano-spaced ligand declustering to stimulate cell adhesion. Tunability of electrodeposition conditions can regulate nanocoil pitch and wire diameter to enable further investigations of the effect of in situ ligand declustering on cell adhesion. Magnetic control of lateral stretchability of nanocoils may be utilized as an electric switch allowing reversible contact between electrodes. Furthermore, this remote control of in situ time-regulated nanocoil stretching can be translated to cytocompatible^[47] in vivo regulation of the mechanosensing-mediated differentiation of stem cells for tissue regeneration.

Supporting Information

Supporting Information is available from the Wiley Online Library or from the author.

Acknowledgements

S.M., M.J.K., and H.J. contributed equally to this work. This work was supported by the National Research Foundation of Korea (NRF) grant funded by the Korea government (MSIT) (No. 2020R1C1C1011038 and 2019R1A2C3006587). HADDF-STEM imaging was conducted with the support of Korea Basic Science Institute. This work was also supported by a Korea University Grant. This work made use of the EPIC facility of Northwestern University’s NUANCE Center, which has received support from the Soft and Hybrid Nanotechnology Experimental (SHyNE) Resource (NSF ECCS-1542205), the MRSEC IRG2 program (NSF DMR-1720139) at the Materials Research Center, the International Institute for Nanotechnology (IIN), the Keck Foundation, and the State of Illinois, through the IIN. The passage 5 human mesenchymal stem cells used in this work were obtained from Lonza.

Conflict of Interest

The authors declare no conflict of interest.

Keywords

in vivo cell adhesion, nanocoil pitch control, remote control, stem cell differentiation, time-regulated ligand stretching

Received: December 11, 2020

Published online:

- [1] C. H. Turner, *Bone* **1998**, *23*, 399.
- [2] K. M. Wisdom, S. L. Delp, E. Kuhl, *Biomech. Model. Mechanobiol.* **2015**, *14*, 195.
- [3] D. MacKenna, S. R. Summerour, F. J. Villarreal, *Cardiovasc. Res.* **2000**, *46*, 257.
- [4] J. S. Lee, Y. H. Roh, Y. S. Choi, Y. Jin, E. J. Jeon, K. W. Bong, S. W. Cho, *Adv. Funct. Mater.* **2019**, *29*, 1807803.
- [5] M. J. Dalby, N. Gadegaard, R. O. C. Oreffo, *Nat. Mater.* **2014**, *13*, 558.
- [6] R. J. C. Bose, N. Tharmalingam, F. J. G. Marques, U. K. Sukumar, A. Natarajan, Y. T. Zeng, E. Robinson, A. Bermudez, E. Chang, F. Habte, S. J. Pitteri, J. R. McCarthy, S. S. Gambhir, T. F. Massoud, E. Mylonakis, R. Paulmurugan, *ACS Nano* **2020**, *14*, 5818.
- [7] W. Li, Z. Q. Yan, J. S. Ren, X. G. Qu, *Chem. Soc. Rev.* **2018**, *47*, 8639.
- [8] B. S. Gomes, B. Simoes, P. M. Mendes, *Nat. Rev. Chem.* **2018**, *2*, 1.
- [9] F. Gong, L. Cheng, N. L. Yang, O. Betzer, L. Z. Feng, Q. Zhou, Y. G. Li, R. H. Chen, R. Popovtzer, Z. Liu, *Adv. Mater.* **2019**, *31*, 1900730.
- [10] L. B. Zhang, Z. J. Wang, J. Das, M. Labib, S. Ahmed, E. H. Sargent, S. O. Kelley, *Angew. Chem., Int. Ed.* **2019**, *58*, 14519.
- [11] Q. Chen, Q. Y. Hu, E. Dukhovlina, G. J. Chen, S. Ahn, C. Wang, E. A. Ogunnaike, F. S. Ligler, G. Dotti, Z. Gu, *Adv. Mater.* **2019**, *31*, 1900192.
- [12] H. Rabie, Y. Zhang, N. Pasquale, M. J. Lagos, P. E. Batson, K. B. Lee, *Adv. Mater.* **2019**, *31*, 1806991.
- [13] H. Kang, K. Y. Zhang, Q. Pan, S. E. Lin, D. S. H. Wong, J. M. Li, W. Y. W. Lee, B. G. Yang, F. X. Han, G. Li, B. Li, L. M. Bian, *Adv. Funct. Mater.* **2018**, *28*, 1802642.
- [14] T. T. Lee, J. R. Garcia, J. I. Paez, A. Singh, E. A. Phelps, S. Weis, Z. Shafiq, A. Shekaran, A. del Campo, A. J. Garcia, *Nat. Mater.* **2015**, *14*, 352.
- [15] Z. Q. Yan, H. S. Qin, J. S. Ren, X. G. Qu, *Angew. Chem., Int. Ed.* **2018**, *57*, 11182.

- [16] W. Li, Z. W. Chen, L. Zhou, Z. H. Li, J. S. Ren, X. G. Qu, *J. Am. Chem. Soc.* **2015**, *137*, 8199.
- [17] L. F. Kadem, M. Holz, K. G. Suana, Q. Li, C. Lamprecht, R. Herges, C. Selhuber-Unkel, *Adv. Mater.* **2016**, *28*, 1799.
- [18] J. I. Giner-Casares, M. Henriksen-Lacey, I. Garcia, L. M. Liz-Marzan, *Angew. Chem., Int. Ed.* **2016**, *55*, 974.
- [19] L. Zwi-Dantsis, B. Wang, C. Marijon, S. Zonetti, A. Ferrini, L. Massi, D. J. Stuckey, C. M. Terracciano, M. M. Stevens, *Adv. Mater.* **2020**, *32*, 1904598.
- [20] M. Prothmann, F. von Knobelsdorff-Brenkenhoff, A. Topper, M. A. Dieringer, E. Shahid, A. Graessl, J. Rieger, D. Lysiak, C. Thalhammer, T. Huelnhagen, P. Kellman, T. Niendorf, J. Schulz-Menger, *PLoS One* **2016**, *11*, e0148066.
- [21] S. Min, Y. S. Jeon, H. J. Jung, C. Khatua, N. Li, G. Bae, H. Choi, H. Hong, J. E. Shin, M. J. Ko, H. S. Ko, I. Jun, H. E. Fu, S. H. Kim, R. Thangam, J. J. Song, V. P. Dravid, Y. K. Kim, H. Kang, *Adv. Mater.* **2020**, *32*, 2004300.
- [22] H. Choi, G. Bae, C. Khatua, S. Min, H. J. Jung, N. Li, I. Jun, H. W. Liu, Y. Cho, K. H. Na, M. Ko, H. Shin, Y. H. Kim, S. Chung, J. J. Song, V. P. Dravid, H. Kang, *Adv. Funct. Mater.* **2020**, *30*, 2001446.
- [23] C. Khatua, S. Min, H. J. Jung, J. E. Shin, N. Li, I. Jun, H. W. Liu, G. Bae, H. Choi, M. J. Ko, Y. S. Jeon, Y. J. Kim, J. Lee, M. Ko, G. Shim, H. Shin, S. Lee, S. Chung, Y. K. Kim, J. J. Song, V. P. Dravid, H. Kang, *Nano Lett.* **2020**, *20*, 4188.
- [24] H. Kang, H. J. Jung, S. K. Kim, D. S. H. Wong, S. Lin, G. Li, V. P. Dravid, L. M. Bian, *ACS Nano* **2018**, *12*, 5978.
- [25] H. Kang, K. Y. Zhang, H. J. Jung, B. G. Yang, X. Y. Chen, Q. Pan, R. Li, X. Y. Xu, G. Li, V. P. Dravid, L. M. Bian, *Adv. Mater.* **2018**, *30*, 1803591.
- [26] S. G. Higgins, M. Becce, A. Belessiotis-Richards, H. Seong, J. E. Sero, M. M. Stevens, *Adv. Mater.* **2020**, *32*, 1903862.
- [27] J. Hu, H. Albadawi, B. W. Chong, A. R. Deipolyi, R. A. Sheth, A. Khademhosseini, R. Oklu, *Adv. Mater.* **2019**, *31*, 1970232.
- [28] H. Kang, S. Kim, D. S. H. Wong, H. J. Jung, S. Lin, K. J. Zou, R. Li, G. Li, V. P. Dravid, L. M. Bian, *Nano Lett.* **2017**, *17*, 6415.
- [29] J. Deng, C. S. Zhao, J. P. Spatz, Q. Wei, *ACS Nano* **2017**, *11*, 8282.
- [30] K. Ye, X. Wang, L. P. Cao, S. Y. Li, Z. H. Li, L. Yu, J. D. Ding, *Nano Lett.* **2015**, *15*, 4720.
- [31] A. R. Hong, Y. Kim, T. S. Lee, S. Kim, K. Lee, G. Kim, H. S. Jang, *ACS Appl. Mater. Interfaces* **2018**, *10*, 12331.
- [32] L. Y. Koo, D. J. Irvine, A. M. Mayes, D. A. Lauffenburger, L. G. Griffith, *J. Cell Sci.* **2002**, *115*, 1423.
- [33] J. H. Huang, S. V. Gräter, F. Corbellini, S. Rinck, E. Bock, R. Kemkemer, H. Kessler, J. D. Ding, J. P. Spatz, *Nano Lett.* **2009**, *9*, 1111.
- [34] J. A. Deeg, I. Louban, D. Aydin, C. Selhuber-Unkel, H. Kessler, J. P. Spatz, *Nano Lett.* **2011**, *11*, 1469.
- [35] J. Xu, S. S. Y. Lee, H. Seo, L. Pang, Y. Jun, R. Y. Zhang, Z. Y. Zhang, P. Kim, W. Lee, S. J. Kron, Y. Yeo, *Small* **2018**, *14*, 1803601.
- [36] T. X. Gu, Y. Wang, Y. H. Lu, L. Cheng, L. Z. Feng, H. Zhang, X. Li, G. R. Han, Z. Liu, *Adv. Mater.* **2019**, *31*, 1806803.
- [37] C. S. Chen, M. Mrksich, S. Huang, G. M. Whitesides, D. E. Ingber, *Science* **1997**, *276*, 1425.
- [38] W. Kim, K. Park, S. J. Yoo, P. Matteini, B. Hwang, B. Kim, S. M. Han, *J. Alloys Compd.* **2020**, *816*, 152586.
- [39] M. Arnold, E. A. Cavalcanti-Adam, R. Glass, J. Blummel, W. Eck, M. Kantlehner, H. Kessler, J. P. Spatz, *ChemPhysChem* **2004**, *5*, 383.
- [40] J.-P. Xiong, T. Stehle, R. Zhang, A. Joachimiak, M. Frech, S. L. Goodman, M. A. Arnaout, *Science* **2002**, *296*, 151.
- [41] J. K. Yoon, M. Misra, S. J. Yu, H. Y. Kim, S. H. Bhang, S. Y. Song, J. R. Lee, S. Ryu, Y. W. Choo, G. J. Jeong, S. P. Kwon, S. G. Im, T. I. Tae, B. S. Kim, *Adv. Funct. Mater.* **2017**, *27*, 1703853.
- [42] K. S. Kim, J. Y. Lee, J. Han, H. S. Hwang, J. Lee, K. Na, *Adv. Funct. Mater.* **2019**, *29*, 1900773.
- [43] K. H. Vining, D. J. Mooney, *Nat. Rev. Mol. Cell Biol.* **2017**, *18*, 728.
- [44] T. C. von Erlach, S. Bertazzo, M. A. Wozniak, C. M. Horejs, S. A. Maynard, S. Attwood, B. K. Robinson, H. Autefage, C. Kallepitis, A. D. Hernandez, C. S. Chen, S. Goldoni, M. M. Stevens, *Nat. Mater.* **2018**, *17*, 237.
- [45] Y. Wei, S. Jiang, M. Si, X. Zhang, J. Liu, Z. Wang, C. Cao, J. Huang, H. Huang, L. Chen, S. Wang, C. Feng, X. Deng, L. Jiang, *Adv. Mater.* **2019**, *31*, 1900582.
- [46] S. Dupont, L. Morsut, M. Aragona, E. Enzo, S. Giullitti, M. Cordenonsi, F. Zanconato, J. L. e Digabel, M. Forcato, S. Bicciato, N. Elvassore, S. Piccolo, *Nature* **2011**, *474*, 179.
- [47] A. Kaushik, R. D. Jayant, R. Nikkhah-Moshiaie, V. Bhardwaj, U. Roy, Z. H. Huang, A. Ruiz, A. Yndart, V. Atluri, N. El-Hage, K. Khalili, M. Nair, *Sci. Rep.* **2016**, *6*, 25309.